

1 Rapid Viral Expansion Beyond the Amazon Basin: Increased Epidemic Activity of 2 Oropouche Virus Across the Americas

3
4 Felipe Campos de Melo Iani^{1^}, Felicidade Mota Pereira^{2^}, Elaine Cristina de Oliveira^{3^}, Janete Taynã
5 Nascimento Rodrigues^{4^}, Mariza Hoffmann Machado^{5^}, Vagner Fonseca^{6-8^}, Talita Emile Ribeiro
6 Adelino^{1,8}, Natália Rocha Guimarães^{1,8}, Luiz Marcelo Ribeiro Tomé^{1,8}, Marcela Kelly Astete Gómez²,
7 Vanessa Brandão Nardy², Adriana Aparecida Ribeiro¹, Alexander Rosewell⁹, Álvaro Gil A. Ferreira⁸,
8 Arabela Leal e Silva de Mello², Brenda Machado Moura Fernandes⁴, Carlos Frederico Campelo de
9 Albuquerque⁹, Dejanira dos Santos Pereira³, Eline Carvalho Pimentel², Fábio Guilherme Mesquita Lima⁴,
10 Fernanda Viana Moreira Silva¹, Glauco de Carvalho Pereira¹, Houriiyah Tegally⁷, Júlia Deffune Profeta
11 Cidin Almeida³, Keldenn Melo Farias Moreno¹⁰, Klaucia Rodrigues Vasconcelos³, Leandro Cavalcante
12 Santos⁴, Lívia Cristina Machado Silva¹, Lívia C. V. Frutuoso¹¹, Ludmila Oliveira Lamounier¹, Mariana
13 Araújo Costa⁴, Marília Santini de Oliveira¹², Marlei Pickler Dediasi dos Anjos⁵, Massimo Ciccozzi¹³,
14 Maurício Teixeira Lima¹⁰, Maira Alves Pereira¹, Marília Lima Cruz Rocha¹, Paulo Eduardo de Souza da
15 Silva¹, Peter Rabinowitz¹⁴, Priscila Souza de Almeida¹, Richard Lessells¹⁵, Ricardo T. Gazzinelli¹⁶, Rivaldo
16 Venâncio da Cunha¹⁷, Sabrina Gonçalves⁵, Sara Cândida Ferreira dos Santos¹, Senele Ana de Alcântara
17 Belettini⁵, Sílvia Helena Sousa Pietra Pedrosa¹, Sofia Isabel Rótulo Araújo⁵, Stephanni Figueiredo da
18 Silva³, Julio Croda^{18,19}, Ethel Maciel²⁰, Wes Van Voorhis²¹, Darren P. Martin²², Edward C. Holmes²³, Tulio
19 de Oliveira²⁴, José Lourenço^{25,26}, Luiz Carlos Junior Alcantara⁸, Marta Giovanetti^{27,28}.

20
21 1. Central Public Health Laboratory of the State of Minas Gerais, Ezequiel Dias Foundation, Brazil; 2.
22 Central Public Health Laboratory of the State of Bahia, Brazil; 3. Central Public Health Laboratory of the
23 State of Mato Grosso, Brazil; 4. Central Public Health Laboratory of the State of Acre, Brazil; 5. Central
24 Public Health Laboratory of the State of Santa Catarina, Brazil; 6. Department of Exact and Earth
25 Sciences, University of the State of Bahia, Salvador, Brazil; 7. Centre for Epidemic Response and
26 Innovation (CERI), School of Data Science and Computational Thinking, Stellenbosch; 8. René Rachou
27 Institute, Oswaldo Cruz Foundation, Belo Horizonte, Brazil University; Stellenbosch, South Africa; 9.
28 Organização Pan-Americana da Saúde, Organização Mundial da Saúde, Brazil; 10. Institute of Biological
29 Sciences, Federal University of Minas Gerais, Belo Horizonte, Brazil; 11. Coordenadora-Geral de
30 Vigilância de Arboviroses, Brazilian Ministry of Health, Brazil; 12. Coordenadora-Geral de Laboratórios de
31 Saúde Pública, Brazilian Ministry of Health, Brazil; 13. Unit of Medical Statistics and Molecular
32 Epidemiology, University Campus Bio-Medico of Rome, Italy; 14. Environmental and Occupational Health
33 Sciences, University of Washington, USA; 15. KwaZulu-Natal Research Innovation and Sequencing
34 Platform (KRISP), Nelson R Mandela School of Medicine, University of KwaZulu-Natal, Durban 4001,
35 South Africa; 16. Fundação Oswaldo Cruz - Minas, Laboratory of Immunopathology, Belo Horizonte, MG,
36 Brazil; 17. Fundação Oswaldo Cruz, Bio-Manguinhos, Rio de Janeiro, Rio de Janeiro, Brazil; 18. Faculdade
37 de Medicina, Universidade Federal de Mato Grosso do Sul, Campo Grande, MS, Brazil; 19. Fundação
38 Oswaldo Cruz - Mato Grosso do Sul, Campo Grande, MS, Brazil; 20. Secretária de Vigilância em Saúde e
39 Ambiente (SVSA - Ministério da Saúde), Brazil; 21. Center for Emerging and Re-emerging Infectious
40 Diseases (CERID), University of Washington; 22. Computational Biology Division, Department of
41 Integrative Biomedical Sciences, Institute of Infectious Disease and Molecular Medicine, Faculty of

42 Health Sciences, University of Cape Town, Cape Town, South Africa; 23. School of Medical Sciences,
43 University of Sydney, Sydney, NSW, Australia; 24. School for Data Science and Computational Thinking,
44 Faculty of Science and Faculty of Medicine and Health Sciences, Stellenbosch University, South Africa;
45 25. Universidade Católica Portuguesa, Católica Medical School, Católica Biomedical Research Centre,
46 Portugal; 26. Climate amplified diseases and epidemics (CLIMADE) Europe, Portugal; 27. Department of
47 Sciences and Technologies for Sustainable Development and One Health, Università Campus Bio-Medico
48 di Roma, Italy; 28. Oswaldo Cruz Institute, Oswaldo Cruz Foundation, Minas Gerais, Brazil.

49

50 ^Denote equal contributions

51

52

53 **Abstract**

54 **Summary:** Oropouche virus (OROV), initially detected in Trinidad and Tobago in 1955, has been
55 historically confined to the Amazon Basin. However, since late 2022, OROV has been reported in
56 northern Brazil as well as urban centers in Bolivia, Colombia, Cuba, and Peru. Herein, we describe the
57 generation of 133 new publicly available full genomes. We show how the virus evolved via genome
58 component reassortment and how it rapidly spread across multiple states in Brazil, causing the largest
59 outbreak ever recorded outside the Amazon basin, including the first detected deaths. This work
60 highlights the need for heightened epidemiological and genomic surveillance and the implementation of
61 adequate measures in order to mitigate transmission and the impacts on the population.

62 **Background:** Oropouche virus was first identified in 1955 in Trinidad and Tobago and later found in
63 Brazil in 1960. Historically, it has been reported to have caused around 30 outbreaks, mostly within the
64 Amazon Basin, where it circulates among forest animals, but also in urban areas where it is known to be
65 transmitted by the midge *Culicoides paraensis*. Recently, Brazil has seen a surge in cases, with more than
66 7000 reported by mid-2024 alone.

67 **Methods:** In a collaboration with Central Public Health Laboratories across Brazilian regions, we
68 integrated epidemiological metadata with genomic analyses of recently sampled cases. This initiative
69 resulted in the generation of 133 whole genome sequences from the three genomic segments (L, M, and
70 S) of the virus, including the first genomes obtained from regions outside the Amazon and from the first
71 ever recorded fatal cases.

72 **Findings:** All of the 2024 genomes form a monophyletic group in the phylogenetic tree with sequences
73 from the Amazon Basin sampled since 2022. Our analyses revealed a rapid north-to-south viral
74 movement from the Amazon Basin into historically non-endemic regions. We identified 21 reassortment
75 events, although it remains unclear if genomic evolution of the virus enabled the virus to adapt to local
76 ecological conditions and evolve new phenotypes of public health importance.

77 **Interpretation:** Both the recent rapid spatial expansion and the first reported fatalities associated with
78 Oropouche (and other outcomes under investigation) underscore the importance of enhancing
79 surveillance for this evolving pathogen across the Region. Without any obvious changes in the human
80 population over the past 2 years, it is possible that viral adaptation, deforestation and recent climate
81 change, either alone or in combination, have propelled Oropouche virus beyond the Amazon Basin.

82

83 **Keywords:** OROV, Brazil, genomic surveillance, Amazon basin.

84 **Research in context.**

85 **Evidence before this study:** Before this study, Oropouche virus (OROV) was known to cause periodic
86 outbreaks primarily within the Amazon Basin. Initially identified in Trinidad and Tobago in 1955, the
87 virus had been responsible for approximately 30 outbreaks in Latin America, mostly confined to the
88 Amazon region. The virus typically circulates among forest animals and is transmitted to humans by the
89 bite of the midge *Culicoides paraensis*. There has been an historical dearth of available genomic data,
90 and so far the spread beyond the Amazon Basin has not been well-documented.

91 **Added value of this study:** This study provides a timely and comprehensive analysis of epidemiological
92 and genomic data of Oropouche virus from regions outside the Amazon Basin. By generating 133 whole
93 genome sequences from various regions across Brazil, this study reveals the movement of OROV over
94 the past few years across Brazil, with a north-south spatial movement from regions of historic
95 endemicity to regions with clear epidemic potential. We identify 21 reassortment events, with the
96 possible occurrence of virus adaptation to new environments. We also report the first fatal cases of
97 Oropouche virus infection in patients without underlying relevant comorbidities, underscoring the public
98 health risk of future outbreaks and the need for increased awareness and surveillance.

99 **Implications of all the available evidence:** The rapid spread of Oropouche virus beyond the Amazon
100 Basin into regions of Brazil more than 3500 Km distant, coupled with the identification of genome
101 reassortment events, raises the possibility that the virus is adapting to the new environments of its
102 increasing spatial landscape. This evolution could lead to the emergence of new viral phenotypes, with
103 potential changes at various levels, from vector efficiency to disease outcome, raising the challenge of
104 managing future outbreaks. This underscores the critical need for enhanced surveillance systems at
105 national and continental levels, particularly in urban centers that appear to have been hit hard during
106 the spatial expansion, to detect and respond to Oropouche virus outbreaks promptly.

107
108 **Introduction**

109 Oropouche virus (OROV; *Orthobunyavirus oropoucheense*) is an arthropod-borne virus classified within
110 the order *Bunyavirales*, family *Peribunyaviridae* and genus *Orthobunyavirus* (1). It is present as a
111 negative-sense, single-stranded RNA genome that is divided into three segments based on size: S
112 (small), M (medium) and L (large). These segments encode four structural proteins: the nucleocapsid,
113 two external glycoproteins, and the RNA polymerase (2). OROV was first identified in 1955 in
114 Oropouche, a village in Trinidad and Tobago (3). Since then, the virus has been responsible for numerous
115 outbreaks, mostly within the Amazon Basin, where it is found among forest animals such as non-human
116 primates, sloths, and birds (4). The midge *Culicoides paraensis* is the primary vector for human
117 transmission. Infection with OROV causes Oropouche fever, which typically presents as fever, headache,
118 muscle and joint pain (5). The majority of human infections present as mild to moderate disease and
119 resolve within a week, although rare cases can lead to complications like aseptic meningoencephalitis
120 (6).

121
122 Historically, OROV outbreaks were largely restricted to the Amazon region, with about 30
123 outbreaks reported in Latin America until recent years (7). However, new epidemiological data show a
124 marked increase in Oropouche fever cases in Brazil, Cuba (N=74), Bolivia (N=356), Colombia (N=74), and

125 Peru (N=290), with travel-related cases reported in Italy, Spain, and Germany, all originating from Cuba,
126 highlighting that it's becoming recognized outside the region (8, 9). Notably, Brazil alone reported a total
127 number of more than 7,000 cases this year (up to August 2024) compared to 836 in 2023, indicating a
128 significant rise in transmission (10-12). In 2024, Brazil also reported the first three fatal cases associated
129 with OROV infection, raising concerns among health authorities (13). OROV has also recently appeared
130 in historically non-endemic Brazilian regions outside the Amazon, including in the far south and,
131 importantly, in some urban centers on the east coast (13). As is the case for other arboviruses (14),
132 recent changes in disease ecology, such as deforestation, urbanization, human mobility and climate
133 change, are some of the possible drivers of its recent emergence in the Amazon region (15). Local
134 reservoir habitats belonging to non-human mammals and vectors can be disrupted, pushing them into
135 closer contact with each other and with urban and peri-urban areas where humans can be infected. In
136 addition, human mobility favors long distance viral movement. Additionally, ongoing changes in OROV
137 genetic diversity may also result in changes in virulence and transmission potential (16).

138
139 Scientific and surveillance data for OROV are currently limited, with fewer than 110 peer-
140 reviewed publications compared to thousands for other arboviruses such as Zika or Dengue (17).
141 Reports of recent increases in OROV epidemic activity underscore the urgent need for more data and
142 research. Some of the epidemic activity over the past decade has provided valuable insights into OROV
143 epidemiological characteristics, as well as its potential for public health impact. To help fill current
144 knowledge gaps in the face of recent epidemic activity in the south of Brazil we, in collaboration with
145 several Central Public Health Laboratories, generated 133 viral genome sequences including all three
146 segments (L, M, and S). Herein, we present genomic analysis that offers insights into OROV's recent
147 movement from northern to southern Brazil and its emergence in regions, within and outside the
148 country, classically not associated with epidemic activity.

149
150 **Methods**

151 **Ethics statement**

152 This project was reviewed and approved by the Ethical Committee of the Federal University of
153 Minas Gerais (CAAE: 32912820.6.1001.5149). The availability of the samples for research purposes
154 during outbreaks of national concern is allowed by the terms of the 510/2016 Resolution of the National
155 Ethical Committee for Research (CONEP - Comissão Nacional de Ética em Pesquisa, Ministério da Saúde)
156 of the Brazilian Ministry of Health (BrMoH), that authorize, without the necessity of an informed
157 consent, the use of clinical samples collected in the Brazilian Central Public Health Laboratories to
158 accelerate knowledge building and contribute to surveillance and outbreak response. The samples
159 processed in this study were obtained anonymously from material collected during routine arboviral
160 diagnosis in Brazilian public health laboratories within the BrMoH network.

161
162
163
164
165

166

167 **Sample collection and molecular diagnostic screening**

168 Clinical samples from patients with suspected OROV infection presenting with acute febrile
169 illness were obtained for routine diagnostic purposes at local health services in five different Brazilian
170 states (Minas Gerais, Bahia, Mato Grosso, Acre and Santa Catarina). Samples were collected between
171 February and May 2024. Viral RNA was extracted from serum samples using an automated protocol, and
172 samples were submitted to a multiplex arbovirus molecular screening by RT-qPCR, including the
173 detection of OROV based on an assay by Naveca et al. (2017) (18). All of these samples yielded positive
174 results only for OROV.

175 **cDNA synthesis and whole genome sequencing**

176 Samples were selected for sequencing based on the CT value (≤ 36) and availability of clinical and
177 epidemiological metadata, such as date of symptom onset, date of sample collection, sex, age,
178 municipality of residence, and symptoms. For cDNA synthesis, the ProtoScript II First Strand cDNA
179 Synthesis kit (NEB) was used following the manufacturer's instructions. The cDNA generated was
180 subjected to multiplex PCR sequencing using Q5 High Fidelity Hot-Start DNA Polymerase (NEB) and a set
181 of specific primers designed by the Zibra Project ([https://github.com/zibraproject/zika-](https://github.com/zibraproject/zika-pipeline/tree/master/schemes/OROV400/V1)
182 [pipeline/tree/master/schemes/OROV400/V1](https://github.com/zibraproject/zika-pipeline/tree/master/schemes/OROV400/V1)) for sequencing the complete genomes of OROV. Whole
183 genome sequencing was performed using both MiSeq (Illumina) and MinION (Oxford Nanopore
184 Technologies) instruments. In the first case, OROV library preparation was carried out using the KAPA
185 HyperPlus kit (Roche), following the manufacturer's instructions. The normalized library was loaded
186 onto a 300-cycle MiSeq Reagent Micro Kit v2 and run on the MiSeq platform (Illumina). For nanopore
187 sequencing, DNA library preparation was performed using the ligation sequencing kit LSK109 (Oxford
188 Nanopore Technologies) and the native barcoding kit EXP-NBD196 (Oxford Nanopore Technologies).
189 Sequencing libraries were loaded into an R9.4 flow cell (Oxford Nanopore Technologies).

190

191 **Generation of consensus sequences**

192 Raw files were basecalled and demultiplexing was done using Guppy v.6.0 (Oxford Nanopore
193 Technologies). Consensus sequences were generated by a hybrid approach using the Genome Detective
194 online tool (<https://www.genomedetective.com/>) (19). The newly generated OROV sequences were
195 deposited in GenBank and will be made available after acceptance.

196

197 **Phylogenetic analysis**

198 Sequences of the 133 complete S, M, and L genomic segments of OROV generated in this study
199 were combined with corresponding segments of all published full-length OROV sequences available in
200 NCBI up to July 2024 (S=376 sequences, M=231 sequences, and L=303 sequences). The sequences from
201 two fatal cases from the state of Bahia (Brazil) collected in March and May 2024, along with one from
202 Mato Grosso, were also included. Sequence alignment of each segment data set was performed using
203 MAFFT (20) and manually curated to remove artifacts using AliView (21). The full genome dataset (with
204 segments concatenated) was checked for potential recombination and reassortment using the program,
205 the RDP5 (using default settings except that segments were considered as linear sequences and window
206 sizes of 16, 50, 40 and 101 were respectively used for the RDP, Chimaera, Maxchi and Bootscan

207 recombination/reassortment detection methods; 22). Genomic regions identified by RDP5 to have been
208 acquired by recombination and genomic segments identified by RDP5 to have been acquired by
209 reassortment, were stripped from the full genome datasets by replacing tracts of sequence acquired
210 through recombination/reassortment with gap characters (“-”) in the alignment file to yield a
211 recombination and reassortment free full genome alignment. The full genome alignment and those of
212 the individual segments were used to infer Maximum Likelihood (ML) phylogenetic trees using IQ-TREE
213 version 2 (23) under the HKY nucleotide substitution model, which was inferred by the ModelFinder
214 application. Branch support was assessed using the approximate likelihood-ratio test based on
215 bootstrap and the Shimodaira–Hasegawa-like procedure with 1,000 replicates.

216 Three different data subsets containing only the 2022-2024 extra-Amazon sequences of S
217 (n=162), M (n=162), and L (n=162) segments, were used to infer spatiotemporal spread patterns from
218 continuous spatially-explicit phylogeographic reconstructions using BEAST v1.10.4 (24). Before
219 phylogeographic analysis, the molecular clock signal in each data subset was assessed using the root-to-
220 tip regression method available in TempEst v1.5.3 (25) following the removal of potential outliers that
221 may violate the molecular clock assumption. We accepted temporal structure when the correlation
222 coefficient was >0.2. We modeled the phylogenetic diffusion and spread of OROV within Brazil by
223 analyzing localized transmission (between Brazilian regions) using a flexible relaxed random walk
224 diffusion model (26) that accommodates branch-specific variation in rates of dispersal, with a Cauchy
225 distribution and a jitter window size of 0.01 (27). For each sequence, latitude and longitude coordinates
226 of the sample were considered. MCMC analyses were set up in BEAST v1.10.4, running in duplicate for
227 50 million interactions and sampling every 10,000 steps in the chain. Convergence for each run was
228 assessed in Tracer v1.7.1 (effective sample size for all relevant model parameters >200) (28). Maximum
229 clade credibility trees for each run were summarized using TreeAnnotator after discarding the initial
230 10% as burn-in. Finally, we used the R package seraphim (29) to extract and map spatiotemporal
231 information embedded in the posterior trees.

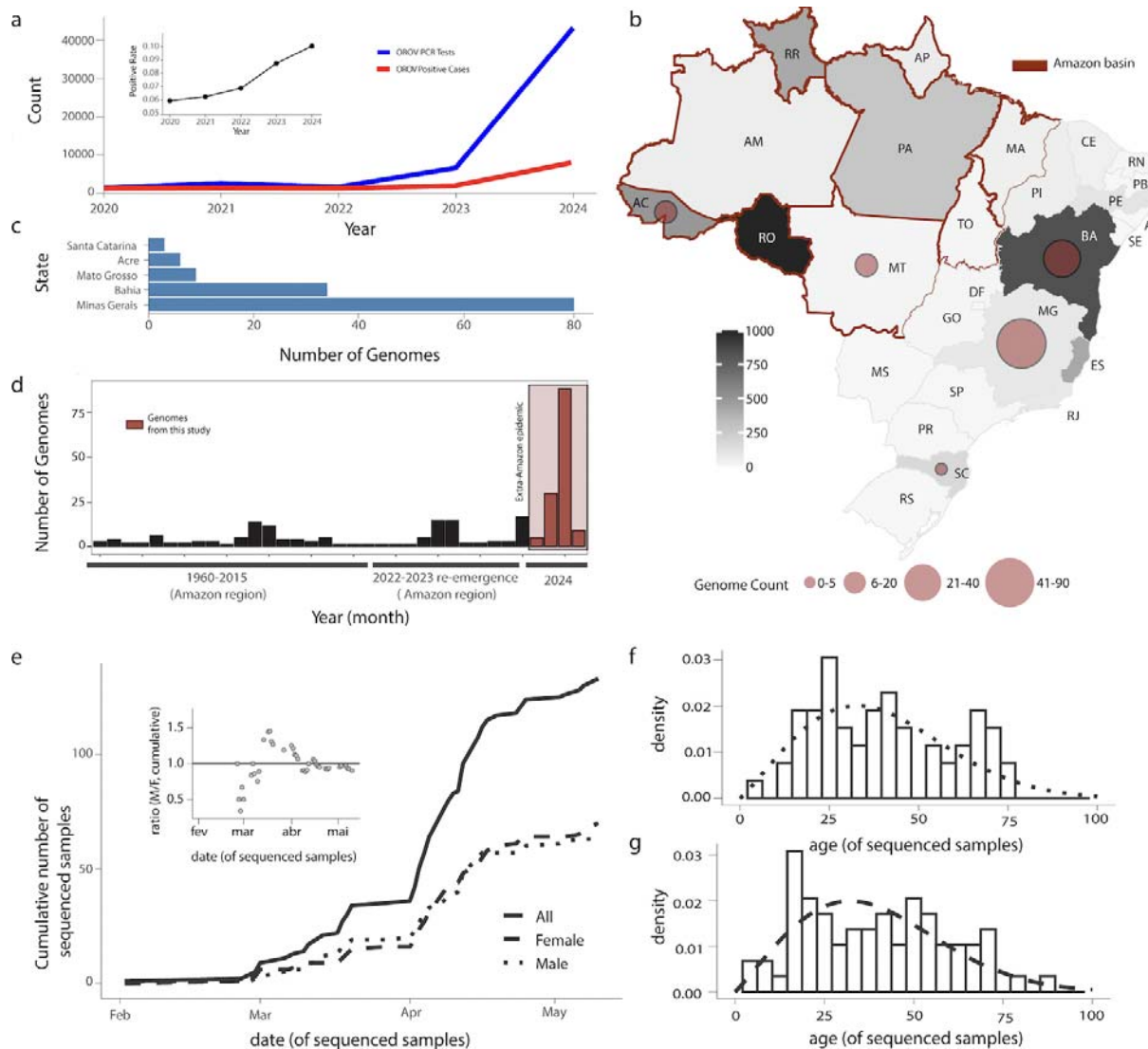
232 To better understand the global dissemination of a specific Brazilian sublineage from 2022-2024,
233 we expanded the data set for each segment to include genome sequences recently isolated in Peru and
234 Italy. We then constructed time-scaled global tree topologies and performed discrete ancestral state
235 reconstruction (of locations) using the *migration* package extension of TreeTime under a GTR model
236 (30). Using a custom Python script, we tracked the number of state changes by iterating over each
237 phylogeny from the root to the external tips. We recorded state changes whenever an internal node
238 transitioned from one country to a different country in its child node or tip(s). The timing of these
239 transition events was documented, providing estimates for import or export events (30).

240
241
242
243
244
245

246
247
248
249
250
251
252
253
254
255
256
257
258
259
260
261
262
263
264
265
266
267
268
269

Results

Between late 2022 and early 2024, the Brazilian states of Acre, Amazonas, Rondônia, and Roraima, located in the western Amazon region, reported a sharp increase in the incidence of OROV human cases (11). Concurrently, there was a substantial increase in the number of real-time RT-PCR tests conducted across the country, reflecting heightened screening efforts (**Figure 1a**). In 2020, initial screening efforts focused primarily on the northern region of Brazil, with the Roraima and Pará states accounting for the majority of the 238 tests conducted (31). At the same time, a few positive cases were detected in Amapá, Amazonas, Pará, Piauí, and Rondônia, signaling the early spread of OROV. By 2021, the number of tests surged to 1,466, with significant increases in states outside the Amazon basin such as Minas Gerais and Ceará. Positive cases were reported predominantly in Amapá, Pará, and Piauí (13). The trend of increased testing continued into 2022, with 588 tests conducted, marking notable expansions in Midwestern and Northeastern Brazilian states. In 2023, the screening efforts intensified further, with 5,280 tests conducted nationwide, with large testing numbers in Bahia, Goiás, Rio de Janeiro, and Tocantins, reflecting widespread concern. Positive cases were detected in multiple states, including Acre, Maranhão, Mato Grosso, Pará, Piauí, Rio Grande do Norte, Rondônia, Roraima, and Tocantins (**Figure 1a**) (13). By early 2024, screening efforts reached an unprecedented level, with 54,428 tests conducted across numerous states (**Figure 1a**). As shown in the inset panel, the positive rate nearly doubled, increasing from 0.059 in 2020 to 0.1 in 2024. The states of Espírito Santo, Minas Gerais, Bahia, and Goiás reported the highest testing numbers outside the Amazon basin (13). Within this period, cumulative positive cases were highest within Rondônia (n=1,747), Bahia (n=837), Espírito Santo (n=416), and Roraima (n=244) (**Figure 1b**).



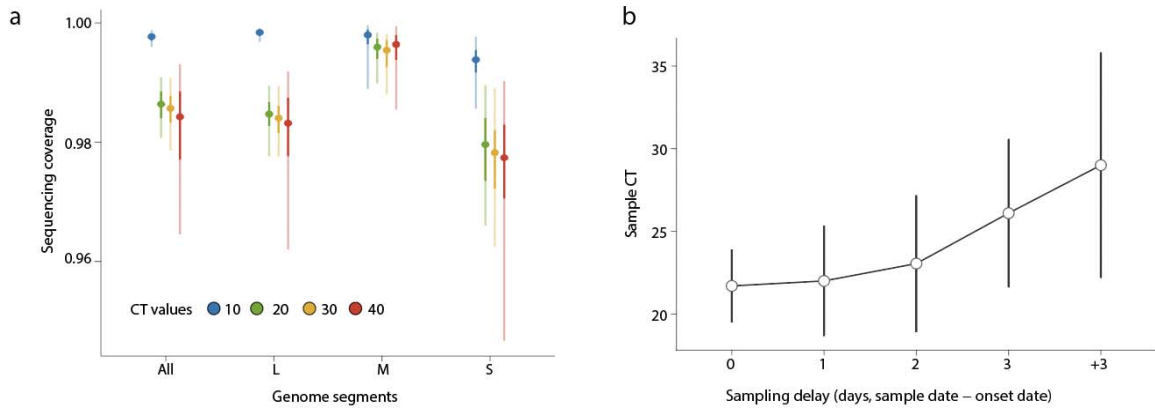
270
 271 **Figure 1. Distribution and Epidemiological Insights of OROV Clinical Cases Detected Beyond the Amazon Basin.** a) Weekly
 272 notified OROV PCR tests and positive cases normalized per 100K individuals per region from 2020 to 2024. The inset panel
 273 shows the positive rate (ratio of positive cases to PCR tests) over the same period, with the y-axis scaled from 0.05 to 0.1 to
 274 highlight the variations; b) Map of Brazil showing the number of new OROV sequences by state. The color and size of the circles
 275 indicates the number of new genomes generated in this study; c) Number of new OROV genomes per state obtained in this
 276 study (Santa Catarina n=3; Acre n=6; Mato Grosso n=9; Bahia n=34; Minas Gerais n=81); d) Number of genomes generated in
 277 this study compared to the number of Brazilian OROV sequences available on the GenBank up to 31st July, 2024. Bars are
 278 months, months with 0 sampling are not shown; e) Cumulative OROV cases in absolute (full line) and by gender (male dotted,
 279 female dashed) of samples from 2024 for which gender metadata was available; the inner panel shows the gender ratio (M/F)
 280 per date; f-g) Observed (bars) and theoretical (lines) age-distributions for males (f) and females (g) of samples from 2024 for
 281 which gender metadata was available. Fitted theoretical distributions were Weibul (male: shape 2.11, scale 44.39, mean 39.15;
 282 female: shape 2.07, scale 44.22, mean 39.16).

283 Five Brazilian states were represented in the 133 newly generated genome sequences: Acre
 284 (N=6, northwest), Bahia (N=34, northeast), Mato Grosso (N=9, midwest), Minas Gerais (N=81, southeast)
 285 and Santa Catarina (N=3, south) (Figure 1c,a). This sampling covered a wide spatial range outside the
 286 Amazon basin (Figure 1a), representing the most time-intensive sampling period to date in Brazil (Figure

287 **1d**). The average cycle threshold (CT) for the three genes was 25, ranging from 8 to 36 (**Table S1**). The
288 gender ratio associated with the genome samples was biased towards females in February-March 2024,
289 but converged to 1 into late local autumn (**Figure 1e**). Cumulatively, 53% (n=70) were female and 47%
290 (n=63) were male (**Table S1**), with genders showing a similar age profile (**Figure 1f-g**). Ages ranged from
291 1 to 89 years, with a median age of ~39 years.

292 Genome sequences were obtained from all five Brazilian macro-regions (North, South,
293 Northeast, South East and North East), revealing north-to-south viral movement across the country
294 (**Figure 1**). The most frequent symptoms observed among the patients were fever, myalgia, and
295 headache. These symptoms were consistently reported across multiple cases, with some patients also
296 experiencing arthralgia. In addition to the common symptomatic presentations, our study identified
297 three fatal cases associated with OROV infection. Notably, these fatalities occurred in young adult
298 patients with no reported comorbidities. In all cases, the clinical course resembled severe dengue, with
299 shock, bleeding, and extensive coagulopathy. Without the extensive lab evaluations due to the ongoing
300 OROV outbreak in the region, these deaths would likely have been misclassified as Dengue Fever rather
301 than OROV. The detection of these fatal cases suggests that OROV may have a broader clinical impact
302 than previously understood, warranting further investigation into the factors contributing to severe
303 disease outcomes. Point mutations were identified in all three fatal cases. In the M segment, amino acid
304 changes included I to V at position 13, M to I at position 642, A to T at position 752, and R to K at
305 position 1342. In the L segment, mutations were found at amino acid positions 857 (T to A), 1634 (K to
306 E), and 2206 (N to D). Further in-depth analyses are required to determine whether these mutations
307 play any role in the pathogenesis and severity of OROV infections. There was seemingly no evidence that
308 symptoms varied with age or gender (**Figure S1**).

309 The sequencing procedures yielded an average coverage of 97.7% for segment S, 98.5% for
310 segment M, and 98.32% for segment L (**Table S1**). Using a Generalized Additive Model similar to the one
311 used for other arboviruses (30), we generated response curves for resulting sequence coverage
312 dependent on sample CT. As expected, both observed (**Table S1**) and estimated sequence coverage
313 were negatively correlated with CT value (**Figure 2a**). Segment M overperformed and segment S
314 underperformed in sequence coverage independently of CT value (albeit only marginally). Segment M
315 was the least sensitive to CT value, showing consistent sequence coverage across sample CT. The states
316 of Bahia and Minas Gerais (~26 and ~61% of samples, respectively) represented extremes of model
317 output, with consistently lower sequence coverage for Bahia and higher coverage for Minas Gerais,
318 independently of sample CT and across all genome segments (**Figure S2**). Prolonged intervals between
319 symptom onset and sample collection were associated with increased CT values (**Figure 2b**), suggesting
320 a decline in viral RNA quantity and consequently sample quality over time, underscoring the critical
321 importance of minimizing the time between symptom onset and sample collection to ensure the
322 acquisition of high-quality sequencing data. Additionally, considering the segmented nature of the OROV
323 genome, we investigated the potential presence of reassortment and recombination among the three
324 different genome segments. We identified 21 reassortment events: 17 separating the S and M
325 segments, 7 separating the S and L segments, and 11 separating the M and L segments.

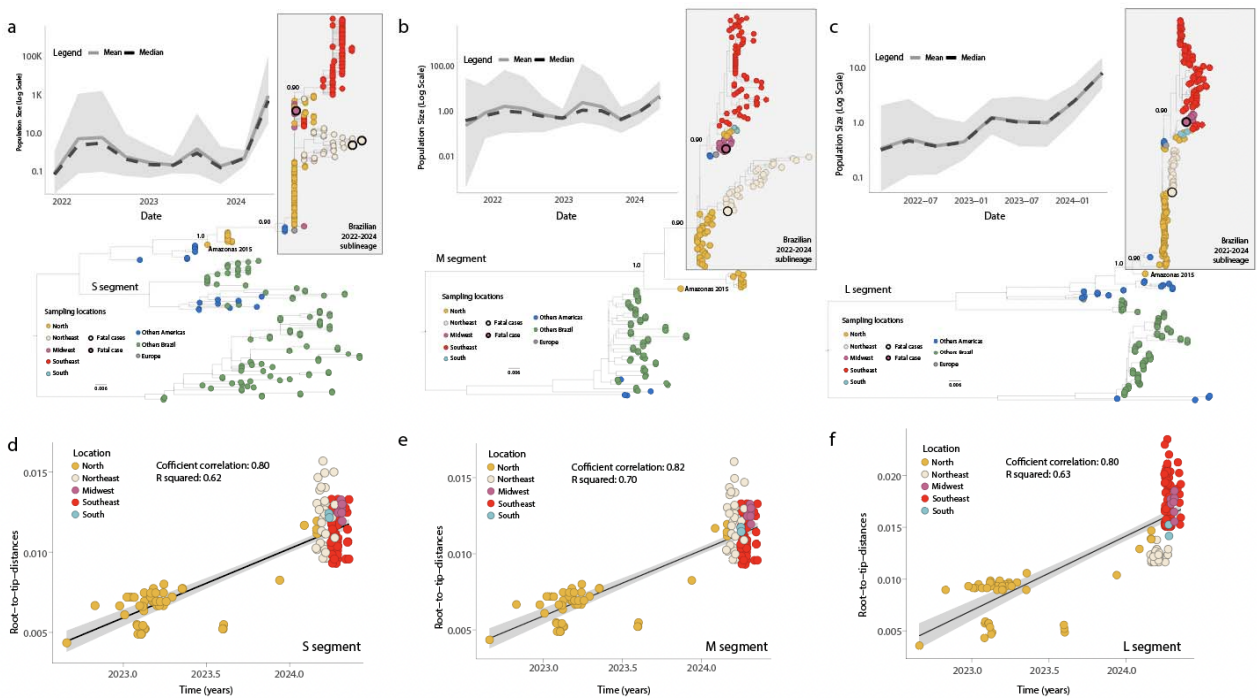


326

327 **Figure 2. Sequencing Coverage and Sample CT Value Analysis: Model Estimates.** a) Summary of estimated sequence coverage
 328 dependent on sample CT using a Generalized Additive Model. Shown are the mean (points) and 95% CI (ranges) for model
 329 estimates given selected values of CT (10, 20, 30, 40, in color) for all segments separately and together; b) Sample CT values
 330 (mean as points, standard deviation as ranges) plotted against the sampling delay (days between symptom onset and sample
 331 collection).

332

333 To reveal the recent evolution of the three OROV genomic segments, we estimated three phylogenetic
 334 trees to determine their relationships with other isolates. Our analysis revealed that the novel OROV
 335 genome sequences sampled in 2024 clustered with sequences from the 2022-2024 epidemic into a
 336 monophyletic group, with strong bootstrap support (values of 1.0) across all three genomic segments
 337 (Figure 3a-c).



338
 339

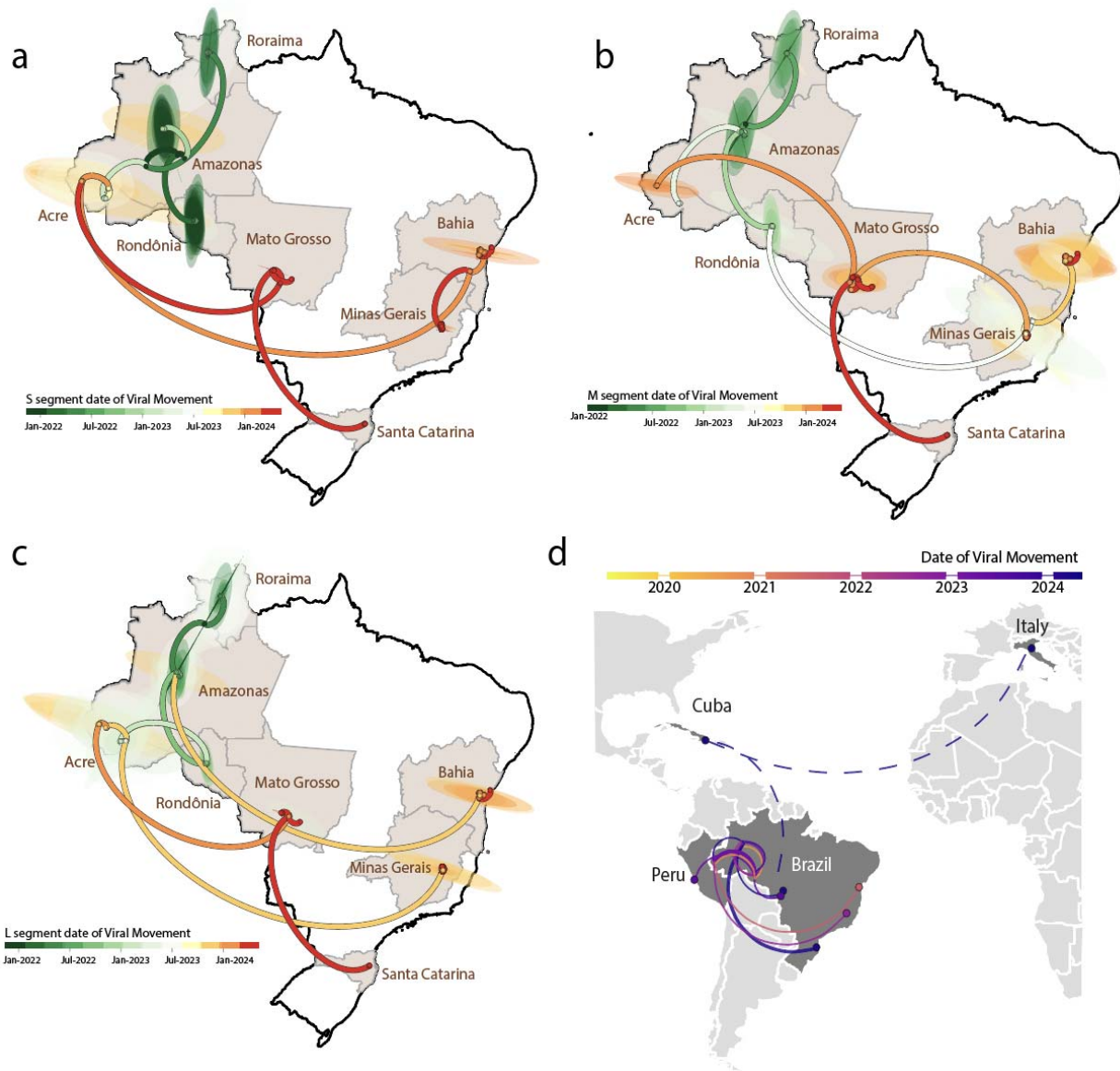
Figure 3. Molecular Evolution and Demographic History of OROV Segments S, M, and L. a- c) Maximum likelihood

340 phylogenetic trees of the three OROV segments: S (n = 376), M (n = 231) (a), L (n = 303). Tips are color-coded according to the
341 legend in the left corner; Inner plots indicate the effective population size (i.e., genetic diversity) of OROV infections (Log scale)
342 over time estimated under the coalescent-based Bayesian Skygrid (BSKG) model (posterior median = solid lines, 95% HPD = pale
343 areas) for each segment; d-f) Regression of sequence sampling dates against root-to-tip genetic distances in a maximum
344 likelihood phylogeny of the Brazilian 2022-2024 expansion clade (n=254).

345 This clade included a basal sequence from the locality of Tefé, Amazonas state, sampled in 2015,
346 indicating a likely Amazonian origin, and has rapidly expanded to other regions, following a north-to-
347 south movement across the country (**Figure 3a-c**). In addition, this lineage has a reassortant
348 evolutionary history, possessing L and S segments from viruses found in Peru, Colombia, and Ecuador
349 and an M segment from viruses detected in the eastern Amazon region. Detailed analysis of the
350 epidemic expansion, based on estimates of effective population size, revealed a sharp increase at the
351 beginning of 2024 (**Figure 3a-c, inner plots**), coinciding with the timing of the national surge in OROV
352 cases (**Figure 1**) (8). In addition, the phylogenetic trees for the S, M, and L segments (**Figure 3a-c**)
353 revealed two main lineages. The first lineage appeared to be primarily composed of sequences from the
354 northern and northeastern regions, while the second lineage was associated with the southeastern and
355 southern regions. This geographical separation might reflect regional diversification of the virus as it
356 spread outside the Amazon basin.

357 The observed topological discordance among the phylogenetic trees of different genomic
358 segments indicated the likelihood of multiple reassortment or recombinant events, supporting the
359 notion that reassortment/recombination is a common and potentially significant evolutionary
360 mechanism in bunyaviruses. A recent preprint manuscript provides more information on the potential
361 reassortment events on genomes from the Amazon Basin (9), so this will not be covered in detail in our
362 manuscript.

363 To reconstruct viral movements across the country, we utilized smaller data sets derived from
364 each genomic segment individually, focusing exclusively on the Brazilian 2022-2024 sublineage (**Figure 3**
365 **a-c**). As there was a strong correlation between sampling time and root-to-tip divergence in all three
366 data sets (**Figure 3 g-i**), we were able to use molecular clock models to infer evolutionary parameters.
367 Accordingly, we estimated that the mean time of origin for this Brazilian 2022-2024 sublineage to be in
368 early November 2021, with a 95% highest posterior density (HPD) interval ranging from early-August
369 2021 to early January 2022. This suggests continuous transmission within the Amazon basin (**Figure 4a-**
370 **c**). Likely introduced in early 2015, this sublineage remained undetected due to insufficient active
371 surveillance at the national level, initially spreading from the northern part of the country (Amazon
372 basin) and subsequently moving towards the northeastern (Bahia state), midwestern (Mato Grosso
373 state), southeastern (Minas Gerais state), and southern (Santa Catarina state) regions (**Figure 4a-c**). We
374 expanded the data set related to this Brazilian 2022-2024 sublineage to include international genome
375 sequences recently isolated in Peru and Italy. Analyses of these data revealed that OROV likely initially
376 moved north to south within Brazil and then crossed borders to reach Peru (**Figure 4d**). Case reports
377 recently detected in Italy are associated with returning travelers from Cuba, although genomes from the
378 latter locality are currently unavailable. It is possible that OROV moved into Cuba sometime in between
379 the events depicted in **Figure 4d** before being exported into Europe.



380

381 **Figure 4. Inferred Viral Dissemination Patterns of OROV in Brazil and Globally.** a-c) Phylogeographic reconstruction of the
 382 spread of OROV (segments S, M, and L) in Brazil. Circles represent nodes of the maximum clade credibility phylogeny and are
 383 colored according to their inferred time of occurrence. Shaded areas represent the 80% highest posterior density interval,
 384 depicting the uncertainty of the phylogeographic estimates for each node. Solid curved lines denote the links between nodes
 385 and the directionality of movement; d) Dissemination patterns of OROV within the Americas and Europe obtained from inferred
 386 ancestral-state reconstructions annotated and colored by region. The destination countries of viral exchange routes are shown
 387 with dots, with curves indicating the routes from the country of origin to the destination country in a counterclockwise
 388 direction. The dashed lines indicate the probable direction of dispersal concluded without evidence due to the paucity of
 389 genomes from Cuba.

390

391

392 Discussion

393 The spread of the novel reassortant OROV lineage between 2022 and 2024 in the Brazilian
394 Amazon region highlights the potential for this virus to emerge and the role of ecological and human
395 factors in its dissemination (11, 12). Our study, along with recent findings (11, 12), underscores the
396 importance of genomic surveillance and phylogenetic analysis in tracing the origin and movement of
397 viral pathogens. The phylogenetic analyses from our study revealed that the OROV sequences sampled
398 between 2022 and 2024 fell into a highly supported monophyletic group, with origins tracing back to a
399 basal sequence from Tefé, Amazonas, Brazil, sampled in 2015. This indicates a likely Amazonian origin
400 for this clade. These findings are consistent with the emergence of a novel reassortant lineage
401 containing the M segment from viruses detected in the eastern Amazon region and the L and S
402 segments from viruses found in Peru, Colombia, and Ecuador (10, 11). This reassortant lineage appears
403 to have emerged in the central region of the Amazonas state between 2010 and 2014, demonstrating a
404 long-range silent dispersion during the latter half of the 2010s. Our study identified approximately 21
405 reassortment events among the different genome segments, supporting the role of reassortment in the
406 evolutionary history of OROV (11). It is possible that this contributed to the virus's ability to adapt to
407 new ecological niches and hosts, fueling its spread across different regions of Brazil. The sharp increase
408 in OROV cases in different Brazilian regions along with the concurrent rise in real-time RT-PCR testing,
409 reflects heightened surveillance and detection efforts underscoring the widespread concern and the
410 proactive measures taken to monitor this emerging pathogen.

411 Our genome-based surveillance approach revealed a clear north-to-south movement of the
412 virus within the country. The peak of OROV transmissions coincided with the rainy season in the Amazon
413 basin, suggesting that environmental factors may play a major role in the virus's transmission dynamics.
414 Deforestation and climate change have contributed to the spread of OROV beyond the Amazon basin
415 (32, 33). The alteration of ecosystems through deforestation disrupts natural habitats and promotes the
416 migration of vectors, such as midges, into new areas (33). Climate change exacerbates this by altering
417 weather patterns and creating favorable conditions for vector proliferation (34). These ecological
418 changes facilitate the movement of OROV from its traditional Amazonian confines to other regions of
419 Brazil and beyond. Recent studies have shown that increased deforestation rates and rising
420 temperatures in the Amazon basin correlate with the expanded range of vector species capable of
421 transmitting OROV (11, 35-40). This north-to-south dissemination pattern highlights the importance of
422 addressing environmental and climate-related factors in controlling the spread of arboviruses. The
423 prolonged cryptic circulation of the virus emphasizes the critical need for robust, active screening
424 programs to monitor and control the spread of such pathogens effectively. The detection of three fatal
425 cases associated with Oropouche virus (OROV) infection, even in patients without reported
426 comorbidities, suggests that the clinical impact of OROV might be more significant than previously
427 understood. This necessitates further investigations into adverse pregnancy outcomes and the potential
428 for vertical transmission of OROV. On August 3rd, the Brazilian Ministry of Health (BrMoH) confirmed
429 the first fetal death due to OROV with mother-to-child transmission in the state Pernambuco, located in
430 the northeastern part of the country (41). This highlights the need for further research into the factors
431 contributing to severe disease outcomes and the development of effective treatment strategies. In

432 addition, the identification of long-range OROV migrations facilitated by human activities, as well as viral
433 expansion beyond Brazilian borders to Peru, Cuba, and subsequently Europe, underscores the global
434 implications of this emerging pathogen. The role of climate change in the expansion of vectors into new
435 regions, coupled with increased human mobility, necessitates a coordinated international response to
436 monitor and control the spread of OROV and other arboviruses.

437 Our study, in conjunction with recent research, emphasizes the critical need for continuous and
438 widespread genomic surveillance. By understanding the evolutionary and epidemiological patterns of
439 OROV, we can better anticipate and mitigate future outbreaks, ensuring more effective public health
440 responses both within Brazil and globally. This approach will be instrumental in managing the ongoing
441 spread of OROV and preparing for potential future threats posed by similar viral pathogens.

442 **Author Contributions:** Conceptualization: V.F., J.L., T.d.O., L.C.J.A., and M.G.; Methodology: F.C.M.I.,
443 F.M.P., E.C.O., J.T.N.R., M.H.M., V.F., T.E.R.A., N.R.G., L.M.R.T., M.K.A.G., V.B.M., A.A.R., A.R., A.G.F.,
444 A.L.S.M., B.M.N.F., C.F.C.A., D.S.P., F.G.M.L., F.V.M.S., G.C.P., H.T., J.D.,P.,C.A., K.M.F.M., K.R.V., L.C.S.,
445 L.C.M.S., L.C.V.F., L.O.M., M.A.C., M.S.O., M.P.D.A., M.C., M.T.L., M.A.P., M.L.C.R., P.E.S.S., P.R., R.S.A.,
446 R.S., R.T.G., R.V.C., S.G., S.C.F.S., S.A.A.B., S.H.S.P.P., S.I.R.A., S.F.S., W.V.V., D.P.M., E.C.H., T.d.O., J.L.,
447 L.C.J.A., and M.G.; Investigation: F.C.M.I., F.M.P., E.C.O., J.T.N.R., M.H.M., V.F., T.E.R.A., N.R.G., L.M.R.T.,
448 M.K.A.G., V.B.M., A.A.R., A.R., A.G.F., A.L.S.M., B.M.N.F., C.F.C.A., D.S.P., F.G.M.L., F.V.M.S., G.C.P., H.T.,
449 J.D.,P.,C.A., K.M.F.M., K.R.V., L.C.S., L.C.M.S., L.C.V.F., L.O.M., M.A.C., M.S.O., M.P.D.A., M.C., M.T.L.,
450 M.A.P., M.L.C.R., P.E.S.S., P.R., R.S.A., R.S., R.T.G., R.V.C., S.G., S.C.F.S., S.A.A.B., S.H.S.P.P., S.I.R.A., S.F.S.,
451 W.V.V., D.P.M., E.C.H., T.d.O., J.L., L.C.J.A., and M.G.; Data curation: V.F., J.L., and M.G.; Original draft
452 preparation: J.L., M.G.; Review and editing: F.C.M.I., F.M.P., E.C.O., J.T.N.R., M.H.M., V.F., T.E.R.A.,
453 N.R.G., L.M.R.T., M.K.A.G., V.B.M., A.A.R., A.R., A.G.F., A.L.S.M., B.M.N.F., C.F.C.A., D.S.P., F.G.M.L.,
454 F.V.M.S., G.C.P., H.T., J.D.,P.,C.A., K.M.F.M., K.R.V., L.C.S., L.C.M.S., L.C.V.F., L.O.M., M.A.C., M.S.O.,
455 M.P.D.A., M.C., M.T.L., M.A.P., M.L.C.R., P.E.S.S., P.R., R.S.A., R.S., R.T.G., R.V.C., S.G., S.C.F.S., S.A.A.B.,
456 S.H.S.P.P., S.I.R.A., S.F.S., W.V.V., D.P.M., E.C.H., T.d.O., J.L., L.C.J.A., and M.G.; Visualization: V.F., J.L.,
457 and M.G. All authors have read and agreed to the published version of the manuscript.

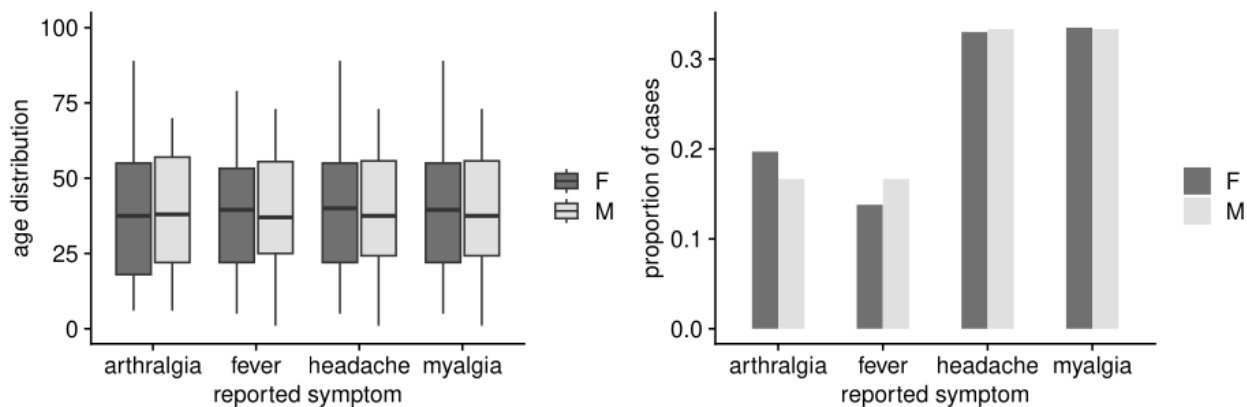
458
459 **Acknowledgments:** This study was supported by the National Institutes of Health USA grant U01
460 AI151698 for the United World Arbovirus Research Network (UWARN), the CRP-ICGEB RESEARCH
461 GRANT 2020 Project CRP/BRA20-03, Contract CRP/20/03, and the Rede Unificada de Análises Integradas
462 de Arbovírus de Minas Gerais (REDE UAI-ARBO-MG), financed by Fundação de Amparo à Pesquisa do
463 Estado de Minas Gerais (FAPEMIG), grant number RED-00234-23. M. Giovanetti's funding is provided by
464 PON "Ricerca e Innovazione" 2014-2020. T.E.R.A. is supported by Conselho Nacional de
465 Desenvolvimento Científico e Tecnológico (CNPq) under the process number 153597/2024-0. F.C.M.I. is
466 supported by FAPEMIG under process number BIP-00123-23. The authors would also like to
467 acknowledge the Global Consortium to Identify and Control Epidemics – CLIMADE
468 (<https://climade.health/>).

469
470 **Conflicts of Interest:** The authors declare no conflict of interest.

471

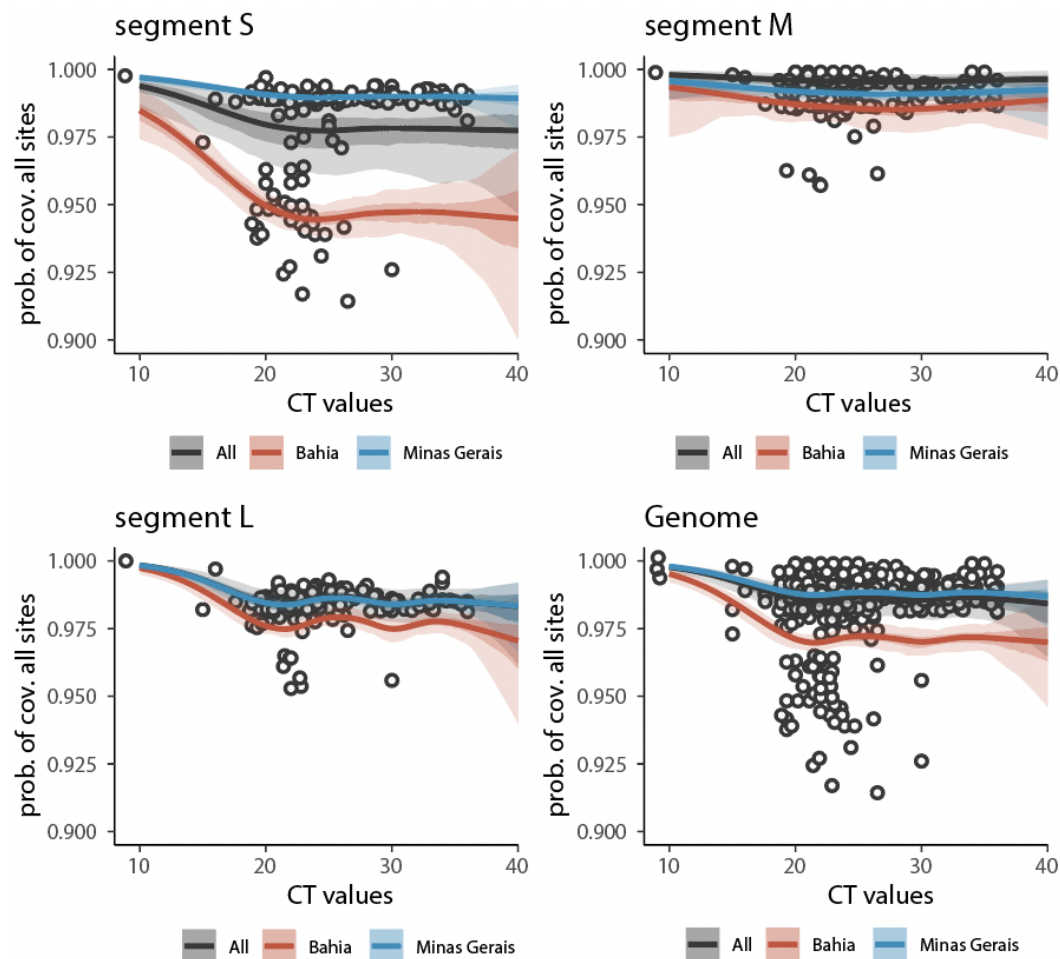
472
473
474
475
476

Supplementary figures



477
478
479
480

Figure S1. Symptoms versus age and gender. The (left) age distribution of cases reported with different symptoms and (b) proportion of cases reporting different symptoms, both disaggregated by gender. Data includes the metadata for the sequenced samples.



481

482 **Figure S2. Sequence Coverage Probability Across Genome Segments in Different Brazilian States.** The figure displays the probability of
483 coverage for all sites across four different genome segments (S, M, L, and the entire genome) in relation to the CT value. The probability was
484 estimated using a Generalized Additive Model (GAM; as done previously e.g. for CHIKV sequencing data [Giovannetti et al Emerg Infect Dis.
485 2023;29(9):1859-1863]). The GAM was defined with a binomial family, with coverage modeled as the proportion of sites recovered from
486 sequencing, using sample state (Brazilian state) as random effect. Solutions presented (in color) include the specific ones for the two states with
487 most sequencing (Bahia, red; Minas Gerais, blue) and the general model output (gray).
488

489 References

- 490
- 491 1. International Committee on Taxonomy of Viruses (ICTV). Available at: <https://ictv.global/taxonomy/>.
492 Accessed on 24 July 2024.
493
- 494 2. Elliott RM. Orthobunyaviruses: recent genetic and structural insights. *Nat Rev Microbiol.* 2014
495 Oct;12(10):673-85. doi: 10.1038/nrmicro3332. Epub 2014 Sep 8. PMID: 25198140.
496
- 497 3. Anderson CR, Spence L, Downs WG, Aitken TH. Oropouche virus: a new human disease agent from
498 Trinidad, West Indies. *Am J Trop Med Hyg.* 1961 Jul;10:574-8. doi: 10.4269/ajtmh.1961.10.574. PMID:
499 13683183.
500
- 501 4. Sakkas H, Bozidis P, Franks A, Papadopoulou C. Oropouche Fever: A Review. *Viruses.* 2018 Apr
502 4;10(4):175. doi: 10.3390/v10040175.
503
- 504 5. Mourão MP, Bastos MS, Gimaque JB, Mota BR, Souza GS, Grimmer GH, Galusso ES, Arruda E,
505 Figueiredo LT. Oropouche fever outbreak, Manaus, Brazil, 2007-2008. *Emerg Infect Dis.* 2009
506 Dec;15(12):2063-4. doi: 10.3201/eid1512.090917.
507
- 508 6. Pinheiro FP, Rocha AG, Freitas RB, Ohana BA, Travassos da Rosa AP, Rogério JS, Linhares AC.
509 Meningite associada às infecções por vírus Oropouche [Meningitis associated with Oropouche virus
510 infections]. *Rev Inst Med Trop Sao Paulo.* 1982 Jul-Aug;24(4):246-51. Portuguese.
511
- 512 7. Vasconcelos HB, Nunes MR, Casseb LM, Carvalho VL, Pinto da Silva EV, Silva M, Casseb SM,
513 Vasconcelos PF. Molecular epidemiology of Oropouche virus, Brazil. *Emerg Infect Dis.* 2011
514 May;17(5):800-6. doi: 10.3201/eid1705.101333.
515
- 516 8. Castilletti C, Mori A, Matucci A, Ronzoni N, Van Duffel L, Rossini G, Sponga P, D'Errico ML, Rodari P,
517 Cristini F, Huits R, Gobbi FG. Oropouche fever cases diagnosed in Italy in two epidemiologically non-
518 related travellers from Cuba, late May to early June 2024. *Euro Surveill.* 2024 Jun;29(26):2400362. doi:
519 10.2807/1560-7917.ES.2024.29.26.2400362. PMID: 38940002; PMCID: PMC11212459.
520
- 521 9. European Centre for Disease Prevention and Control (ECDC), 2024.
522 <https://www.ecdc.europa.eu/sites/default/files/documents/2024-WCP-0037%20Final.pdf>
523

- 524 10. Pan American Health Organization (PAHO). Epidemiological Alert Oropouche in the Region of the
525 Americas: vertical transmission event under investigation in Brazil (2024). Available on
526 [https://www.paho.org/pt/documentos/alerta-epidemiologica-oropouche-na-regiao-das-americas-](https://www.paho.org/pt/documentos/alerta-epidemiologica-oropouche-na-regiao-das-americas-evento-transmissao-vertical-sob)
527 [evento-transmissao-vertical-sob](https://www.paho.org/pt/documentos/alerta-epidemiologica-oropouche-na-regiao-das-americas-evento-transmissao-vertical-sob). Accessed on 03 August 2024.
528
- 529 11. Naveca F., et al., Emergence of a novel reassortant Oropouche virus drives persistent human
530 outbreaks in the Brazilian Amazon region from 2022 to 2024. MedRxiv,
531 <https://doi.org/10.1101/2024.07.23.24310415>.
532
- 533 12. Scachetti et al., Reemergence of Oropouche virus between 2023 and 2024 in Brazil.
534 MedRxiv,<https://doi.org/10.1101/2024.07.27.24310296>.
535
- 536 13. Brazilian Ministry of Health. Oropouche fever. [https://www.gov.br/saude/pt-br/assuntos/saude-de-](https://www.gov.br/saude/pt-br/assuntos/saude-de-a-a-z/a/arboviroses/informe-diario)
537 [a-a-z/a/arboviroses/informe-diario](https://www.gov.br/saude/pt-br/assuntos/saude-de-a-a-z/a/arboviroses/informe-diario).
538
- 539 14. Giovanetti M, Pinotti F, Zanluca C, Fonseca V, et al. Genomic epidemiology unveils the dynamics and
540 spatial corridor behind the Yellow Fever virus outbreak in Southern Brazil. *Sci Adv*. 2023
541 Sep;9(35):eadg9204. doi: 10.1126/sciadv.adg9204. Epub 2023 Sep 1. PMID: 37656782; PMCID:
542 PMC10854437.
543
- 544 15. Pan American Health Organization (PAHO). Public Health Risk Assessment related to Oropouche
545 Virus (OROV) in the Region of the Americas (2024). Available on
546 [https://www.paho.org/en/documents/public-health-risk-assessment-related-oropouche-virus-orov-](https://www.paho.org/en/documents/public-health-risk-assessment-related-oropouche-virus-orov-region-americas-9-february)
547 [region-americas-9-february](https://www.paho.org/en/documents/public-health-risk-assessment-related-oropouche-virus-orov-region-americas-9-february). Accessed on 03 August 2024.
548
- 549 16. Bandeira AC, Barbosa ACFN, Souza M, Saavedra RC, et al. Clinical profile of Oropouche Fever in
550 Bahia, Brazil: unexpected fatal cases. *Scielo Preprints*, 2024. doi: 10.1590/SciELOPreprints.9342.
551
- 552 17. Wesselmann KM, Postigo-Hidalgo I, Pezzi L, de Oliveira-Filho EF, Fischer C, de Lamballerie X, Drexler
553 JF. Emergence of Oropouche fever in Latin America: a narrative review. *Lancet Infect Dis*. 2024
554 Jul;24(7):e439-e452. doi: 10.1016/S1473-3099(23)00740-5. Epub 2024 Jan 25. PMID: 38281494.
555
- 556 18. Naveca FG, Nascimento VAD, Souza VC, Nunes BT, Rodrigues DSG, Vasconcelos PFDC. Multiplexed
557 reverse transcription real-time polymerase chain reaction for simultaneous detection of Mayaro,
558 Oropouche, and Oropouche-like viruses. *Mem Inst Oswaldo Cruz*. 2017 Jul;112(7):510-513. doi:
559 10.1590/0074-02760160062.
560
- 561 19. Vilsker M, Moosa Y, Nooij S, Fonseca V, Ghysens Y, Dumon K, Pauwels R, Alcantara LC, Vanden
562 Eynden E, Vandamme AM, Deforche K, de Oliveira T. Genome Detective: an automated system for virus
563 identification from high-throughput sequencing data. *Bioinformatics*. 2019 Mar 1;35(5):871-873. doi:
564 10.1093/bioinformatics/bty695.
565

- 566 20. Katoh K, Standley DM. MAFFT multiple sequence alignment software version 7: improvements in
567 performance and usability. *Mol Biol Evol.* 2013 Apr;30(4):772-80. doi: 10.1093/molbev/mst010.
568
- 569 21. Larsson A. AliView: a fast and lightweight alignment viewer and editor for large datasets.
570 *Bioinformatics.* 2014 Nov 15;30(22):3276-8. doi: 10.1093/bioinformatics/btu531.
571
- 572 22. Martin DP, Varsani A, Roumagnac P, Botha G, Maslamoney S, Schwab T, Kelz Z, Kumar V, Murrell B.
573 RDP5: a computer program for analyzing recombination in, and removing signals of recombination from,
574 nucleotide sequence datasets. *Virus Evol.* 2020 Apr 12;7(1):veaa087. doi: 10.1093/ve/veaa087.
575
- 576 23. Minh BQ, Schmidt HA, Chernomor O, Schrempf D, Woodhams MD, von Haeseler A, Lanfear R. IQ-
577 TREE 2: New Models and Efficient Methods for Phylogenetic Inference in the Genomic Era. *Mol Biol Evol.*
578 2020 May 1;37(5):1530-1534. doi: 10.1093/molbev/msaa015. Erratum in: *Mol Biol Evol.* 2020 Aug
579 1;37(8):2461. doi: 10.1093/molbev/msaa131.
580
- 581 24. Suchard MA, Lemey P, Baele G, Ayres DL, Drummond AJ, Rambaut A. Bayesian phylogenetic and
582 phylodynamic data integration using BEAST 1.10. *Virus Evol.* 2018 Jun 8;4(1):vey016. doi:
583 10.1093/ve/vey016.
584
- 585 25. Rambaut A, Lam TT, Max Carvalho L, Pybus OG. Exploring the temporal structure of heterochronous
586 sequences using TempEst (formerly Path-O-Gen). *Virus Evol.* 2016 Apr 9;2(1):vew007. doi:
587 10.1093/ve/vew007.
588
- 589 26. Lemey P, Rambaut A, Welch JJ, Suchard MA. Phylogeography takes a relaxed random walk in
590 continuous space and time. *Mol Biol Evol.* 2010 Aug;27(8):1877-85. doi: 10.1093/molbev/msq067.
591
- 592 27. Dellicour S, Gill MS, Faria NR, Rambaut A, Pybus OG, Suchard MA, Lemey P. Relax, Keep Walking - A
593 Practical Guide to Continuous Phylogeographic Inference with BEAST. *Mol Biol Evol.* 2021 Jul
594 29;38(8):3486-3493. doi: 10.1093/molbev/msab031.
595
- 596 28. Rambaut A, Drummond AJ, Xie D, Baele G, Suchard MA. Posterior Summarization in Bayesian
597 Phylogenetics Using Tracer 1.7. *Syst Biol.* 2018 Sep 1;67(5):901-904. doi: 10.1093/sysbio/syy032.
598
- 599 29. Dellicour S, Rose R, Faria NR, Lemey P, Pybus OG. SERAPHIM: studying environmental rasters and
600 phylogenetically informed movements. *Bioinformatics.* 2016 Oct 15;32(20):3204-3206. doi:
601 10.1093/bioinformatics/btw384.
602
- 603 30. Giovanetti, M., Slavov, S.N., Fonseca, V. et al. Genomic epidemiology of the SARS-CoV-2 epidemic in
604 Brazil. *Nat Microbiol* 7, 1490–1500 (2022). <https://doi.org/10.1038/s41564-022-01191-z>.
605
- 606 31. Brazilian Ministry of Health, Oropouche fever. [https://www.gov.br/saude/pt-br/assuntos/saude-de-](https://www.gov.br/saude/pt-br/assuntos/saude-de-a-a-z/o/oropouche/painel-epidemiologico)
607 [a-a-z/o/oropouche/painel-epidemiologico](https://www.gov.br/saude/pt-br/assuntos/saude-de-a-a-z/o/oropouche/painel-epidemiologico)

- 608
609 32. Burkett-Cadena ND, Vittor AY. Deforestation and vector-borne disease: Forest conversion favors
610 important mosquito vectors of human pathogens. *Basic Appl Ecol.* 2018 Feb;26:101-110. doi:
611 10.1016/j.baae.2017.09.012. Epub 2017 Sep 23. PMID: 34290566; PMCID: PMC8290921.
612
- 613 33. Lorenz C, de Oliveira Lage M, Chiaravalloti-Neto F. Deforestation hotspots, climate crisis, and the
614 perfect scenario for the next epidemic: The Amazon time bomb. *Sci Total Environ.* 2021 Aug
615 20;783:147090. doi: 10.1016/j.scitotenv.2021.147090. Epub 2021 Apr 14. PMID: 33872911; PMCID:
616 PMC8721566.
617
- 618 34. Ellwanger JH, Kulmann-Leal B, Kaminski VL, Valverde-Villegas JM, Veiga ABGD, Spilki FR, Fearnside
619 PM, Caesar L, Giatti LL, Wallau GL, Almeida SEM, Borba MR, Hora VPD, Chies JAB. Beyond diversity loss
620 and climate change: Impacts of Amazon deforestation on infectious diseases and public health. *An Acad*
621 *Bras Cienc.* 2020 Apr 17;92(1):e20191375. doi: 10.1590/0001-3765202020191375. PMID: 32321030.
622
- 623 35. Rocklöv, J., Dubrow, R. Climate change: an enduring challenge for vector-borne disease prevention
624 and control. *Nat Immunol* 21, 479–483 (2020). <https://doi.org/10.1038/s41590-020-0648-y>
625
- 626 36. Nunes, M. R. T., Silva, S. P., Carvalho, V. L., Vasconcelos, J. M., Da Silva, D. E. A., & Oliveira, L. F. et al.
627 Emergence of new insect-restrictive viruses in the Amazon region. *Genome Announcements*, 2016; 3(2):
628 e00131-15. doi:10.1128/genomeA.00131-15.
629
- 630 37. Lowe, R. et al. Tackling climate change and deforestation to protect against vector-borne diseases.
631 *Nature Microbiology*, 2023; 8, 2220–2222. doi:10.1038/s41564-023-01533-5.
632
- 633 38. Bloomfield, L. S. P., McIntosh, T. L., & Lambin, E. Why deforestation and extinctions make pandemics
634 more likely. *Nature*, 2020. <https://www.nature.com/articles/d41586-020-02341-1>.
635
- 636 39. Vittor, A. Y. et al. Deforestation can facilitate the emergence and spread of some infectious
637 diseases."Climate Feedback, 2009. [https://climatefeedback.org/deforestation-can-facilitate-the-](https://climatefeedback.org/deforestation-can-facilitate-the-emergence-and-spread-of-some-infectious-diseases)
638 [emergence-and-spread-of-some-infectious-diseases](https://climatefeedback.org/deforestation-can-facilitate-the-emergence-and-spread-of-some-infectious-diseases).
639
- 640 40. Jones, K. E., Patel, N. G., Levy, M. A., Storeygard, A., Balk, D., Gittleman, J. L., & Daszak, P. Global
641 trends in emerging infectious diseases. *temp Nature*, 2008; 451(7181), 990-993.
642 doi:10.1038/nature06536.
643
- 644 41. Brazilian Ministry of Health, 2024. [https://www.gov.br/saude/pt-](https://www.gov.br/saude/pt-br/assuntos/noticias/2024/agosto/saude-confirma-um-obito-fetal-por-oropouche-em-pernambuco)
645 [br/assuntos/noticias/2024/agosto/saude-confirma-um-obito-fetal-por-oropouche-em-pernambuco](https://www.gov.br/saude/pt-br/assuntos/noticias/2024/agosto/saude-confirma-um-obito-fetal-por-oropouche-em-pernambuco)
646